N.A.E.

R. & M. No. 2694
(12,324)
A.R.C. Technical Report

MINISTRY OF SUPPLY

AERONAUTICAL RESEARCH COUNCIL
REPORTS AND MEMORANDA

Some Tests on Compressor Cascades of Related Aerofoils having Different Positions of Maximum Camber

By

A. D. S. CARTER

LONDON: HER MAJESTY'S STATIONERY OFFICE
1953
FIVE SHILLINGS NET

Some Tests on Compressor Cascades of Related Aerofoils having Different Positions of Maximum Camber

By

A. D. S. CARTER

COMMUNICATED BY THE PRINCIPAL DIRECTOR OF SCIENTIFIC RESEARCH (AIR), MINISTRY OF SUPPLY

Reports and Memoranda No. 2694*

December, 1948

Summary.—One of the major variables defining the shape of any blade is its position of maximum camber, and there are several indications that its choice considerably effects the performance of the cascade. Tests have therefore been carried out on a series of aerodynamically equivalent cascades in which the position of maximum camber was varied systematically. The tests covered a full incidence range up to choking. From the results and consideration of other work the following conclusions were reached.

(1) Bringing the position of maximum camber forward gives a wider working range and a higher choking mass flow.

(2) Moving the position of maximum camber back gives a higher work capacity and a higher drag critical Mach number.

(3) With the present design rules there can be little doubt that the best all-round performance is obtained with blades having their positions of maximum camber 50 per cent of the chord from the leading edge provided adequate throat area can be provided with this design.

(4) With improved methods of design it is anticipated that the performance for the other positions of maximum camber could be improved, but even so the best combination of large working range and good high-speed performance appears to occur for a blade having its position of maximum camber as in (3) above.

These conclusions apply to the two-dimensional performance of a cascade of blades : in an actual compressor the results may have to be modified to accommodate the three-dimensional nature of the flow.

1. *Introduction.*—The use of the axial compressor as a component of the aircraft gas turbine has resulted in constant endeavours to reduce its weight. One method of achieving this is to use higher velocities through the cascades of the compressor, and consequently obtain higher stage temperature rises. There is, unfortunately, a limit to which velocities or Mach numbers can be increased without incurring a serious fall off in efficiency due to shock stalling of the blades, and in an attempt to keep this upper limit as high as possible various different profiles have been suggested for compressor blades[1,2]. For a given deflection and air outlet angle, the major parameters defining the profile are the position of maximum camber, the position of maximum thickness, and the value of the maximum thickness itself. Of these the most important is probably the latter, but there is indication that the first of the parameters can have a substantial effect on the performance of a cascade. Consequently a series of tests were undertaken on a representative design of cascade in which the position of maximum camber was varied to cover the complete range likely to be encountered in practise.

* N.G.T.E. Report R.47, received 2nd May, 1949.

2. *Notation and Definitions.*—Standard notation has been used throughout this report.

From practical considerations the following definitions have been adopted :—

Stalling Incidence is that incidence at which the total-head loss becomes twice its minimum value.

Critical Mach Number is the stream Mach number at which sonic velocity is first reached locally at some point on the aerofoil.

Drag Critical Mach Number is the stream Mach number at which the total-head loss becomes $1 \cdot 5$ times its minimum value at that incidence.

Maximum Mach Number is the stream Mach number corresponding to zero pressure rise across the cascade.

3. *Apparatus.*—3.1. *No. 6 High Speed Cascade Wind Tunnel.*—A photograph of No. 6 High Speed Cascade Wind tunnel, the one used for these tests, is given in Fig. 1. The cascade is mounted between two large end plates (one of these has been removed in Fig. 1a to show the cascade), which also carry the traversing gear, static tappings, etc. This assembly is carried by two trunnions fixed to the inlet section of the wind-tunnel as shown in the photographs, the axis of rotation coinciding with the leading edge of the first blade of the cascade. The two side walls are also attached to the inlet section : one is permanently fixed with its tip in contact with the leading edge of the first blade of the cascade, while the other is adjustable in two directions at right-angles. The adjustable wall is clearly visible in Fig. 1a.

The incidence of the cascade can be adjusted by rotating the cascade-traverse gear assembly about the leading edge of the first blade, which remains continually in contact with the fixed side wall. The tip of the adjustable wall is then lined up with the leading edge of the appropriate blade at the other end of the cascade, and the complete unit locked in position by two clamping plates as shown in Fig. 1b.

The working-section of the wind-tunnel varies between $3 \cdot 35$ in. $\times$ $2 \cdot 25$ in. and $4 \cdot 35$ in. $\times$ $2 \cdot 25$ in. measured perpendicular to the inlet flow direction. At a pitch/chord ratio of unity and using the normal $\frac{3}{4}$-in. chord blades, this allows seven blades to be placed in the working-section at an inlet angle of 20 deg increasing to sixteen blades at an angle of 70 deg. The $2 \cdot 25$-in. blade height and $0 \cdot 75$-in. chord give an aspect ratio of $3 \cdot 0$. Boundary-layer suction on this tunnel is optional, the plain side-wall tips shown in Fig. 1a being replaced by slotted ones. However, suction was not used in these tests, the larger number of blades at the higher inlet angles enabling constant conditions to be maintained over the centre blades.

For the majority of the tests a temporary set-up was adopted, the air being accelerated from a 10-in. diameter pipe into the tunnel, and discharged freely to atmosphere. Fifteen diameters of settling length was allowed before the accelerator. The tunnel was later transferred to its permanent home, which is shown in Fig. 2. Extensive checking was carried out, and it was established that with stable conditions loss measurements could be repeated to within 10 per cent of themselves and angles to within $0 \cdot 5$ deg. With the unstable conditions encountered near the stalling-point readings could not be repeated to this degree of accuracy, but it is extremely doubtful if any value can be quoted under these conditions.

The air flow pattern at entry to the cascade was considered reasonably good. A contour plot of the velocity distribution at inlet to the cascade is shown in Fig. 3 for a representative air inlet angle of $47 \cdot 8$ deg. Sectional plots of the velocity along the centre-line of the cascade and along the blade height are also given. The conditions for other air inlet angles and Mach numbers were very similar to the one given in this example.

4. *The Cascades.*—4.1. *Aerodynamic Design.*—The series of blades tested were designed so as to be aerodynamically equivalent, *i.e.*, they were all designed for the same nominal air outlet angle and all had the same blade inlet angle. For a given air inlet angle the incidence was, therefore, the same on all blades, the design being such as to give nominal conditions at zero incidence. The pitch/chord ratio was unity in all cases.

The camber line was a parabolic arc and the position of maximum camber was increased from 30 per cent of the chord from the leading edge to 60 per cent in equal increments, as indicated in Table 1. The C.4 base profile was superimposed on each of these camber lines, this being the one normally used in axial compressors.

An additional blade having the C.1 base profile on a circular-arc camber line was also tested for comparison purposes. This blade is almost identical with the parabolic-arc cambered blade having its position of maximum camber 50 per cent from the leading edge.

The design clearly necessitates a knowledge of the deviation to be expected from each of the cascades. At the time of design the rule from R. & M. 2095[3] was in everyday use, viz.,

$$\delta = m\theta\sqrt{(s/c)}\left(x_2 - \tan^{-1}\frac{b}{c-a}\right).$$

The more accurate rule of R. & M. 2384[2] had not then been formulated with the result that the actual measured air outlet angles are not exactly equal to the design value of 15 deg. The error is, however, very small for these cascades, and it is not considered that the conclusions are in any way affected.

Details of the cascades, using standard notation, are given below. The profiles and passages for each of the cascades are given in Figs. 4 and 5.

TABLE 1

Aerofoil	*Stagger*	*Pitch/Chord*
10C4/31·5 P30	−17·2	1·0
10C4/36 P40	−21·4	1·0
10C4/40 P50	−24·6	1·0
10C4/51 P60	−28·7	1·0
10C1/40 C50	−24·6	1·0

The blades had a $\frac{3}{4}$-in. chord so that for the test conditions the Reynolds number was approximately 2×10^5 at a Mach number of $0 \cdot 5$, but this has to be multiplied by a turbulence factor to get the effective Reynolds number. This could not be determined easily but is at least $2 \cdot 0$.

4.2. *General Manufacture and Inspection.*—The blades used for these tests were machined from nickel-chrome steel. They had an 0·75-in. chord and a 2·25-in. span, the roots being machined integral with the blades. The contour of the blades at the mid-span position was checked by projecting the sections up to twenty times full size. Some projections for a representative set of blades have been reproduced in Fig. 6. It will be noticed that the profiles have reasonably good leading and trailing edges. The maximum error on the blades tested was less than 0·003 in. The figure also shows the difference between the C.4 profile on a parabolic-arc camber line and the C.1 profile on a circular-arc camber line.

5. *Test Results.*—5.1. *General.*—The performance characteristics are given in Figs. 7 to 11 for each of the cascades tested. They have been plotted as total-head loss and deflection against air inlet angle, in the normal manner. The inlet angle corresponding to zero incidence, and therefore the design point, has been indicated in each case. In Figs. 12 and 13 the drag critical and maximum Mach numbers have also been plotted against inlet angle for each of the cascades. Full details of the test values from which these curves were plotted are given in Appendix II for reference purposes.

In two cases the testing was carried on well into the stalled region in order to obtain some idea of the stage performance in a badly matched compressor. This testing was confined to the more practical sections (maximum camber at 40 per cent and 50 per cent of the chord from the leading edge) as severe vibrations were often encountered under these conditions, particularly at high Mach numbers. Examination of the traverses showed that the ‘ ledge ’ in the loss curve at high incidences occurs when the wake has spread right across the passage, the flow having broken away completely from the upper surface. All the work is probably being done by the lower surface at this point. With further increase of incidence the wake from the upper surface is possibly interfering with the flow on the lower surface of the adjacent blade, and a steady increase of loss with incidence follows.

A comparison of the results for the two blades having their position of maximum camber at 50 per cent chord from their leading edges can be obtained from Figs. 9 and 11. The characteristics are substantially the same, except that the deviation for the 10C4/40 P50 blade is some $1 \cdot 5$ deg greater than for 10C1/40 C50. This is probably due to the differences in the blade sections as shown in Fig. 6 though it does appear to be rather large for these changes. The 10C4/40 P50 blade also has a slightly lower stalling incidence, especially at high Mach numbers, but it is impossible to say whether this is due to the thicker trailing edge, or to the somewhat poor profile at the leading edge of this blade (*see* Fig. 6).

A direct comparison between the performance of each of the cascades of the series is, unfortunately, not possible. Referring to Figs. 7 to 10, it will be seen that the design conditions have not been fully satisfied by all the cascades. There is a very definite tendency for the working range to move to more negative incidences as the position of maximum camber is brought forward towards the leading edge; in fact, for the extreme case when the position of maximum camber is 30 per cent from the leading edge the blade is completely stalled at the design point. Since in consequence of this the cascades are not aerodynamically equivalent it is necessary to define a new working point at which comparisons of performance can be made. For the purpose of this report the new working point has been taken as the incidence corresponding to maximum lift/drag conditions at a Mach number of $0 \cdot 4$.

5.2. *Discussion of Results.*—The relative performance of the series has been summarised in Fig. 14 where each of the major characteristics has been plotted against the position of maximum camber. The most important feature is undoubtedly the reduction of optimum incidence as the position of maximum camber is brought forward. It would appear from these tests that the design criteria for blades with their position of maximum camber at positions other than mid-chord will need considerable revision. It is hardly possible to generalise from the single series of tests reported here, but until further information becomes available it is suggested that cambers should be increased, or nominal deflections decreased, so as to give the same relative incidence as in Fig. 14.

While it may be possible with an improved design rule to obtain optimum performance at the design point, the decreasing values of the lift/drag ratios at either end of the range should not be ignored. Here again this decrease of efficiency may be a condemnation of the original design rule rather than the type of blade, but it is not considered insignificant that the maximum possible value of the lift/drag ratio occurs with the type of blade for which the working point is roughly at zero incidence, *i.e.*, $a/c = 53$ per cent in Fig. 14.

One advantage to be gained by bringing the position of maximum camber forward appears to be the increase of the unstalled incidence range as shown in Fig. 14. This may be of considerable importance in combating some of the unknown factors introduced by the three-dimensional nature of the flow in an actual compressor. But it is to be noticed that at high speeds this phenomenon is not so pronounced due to the shock stall curtailing the low-speed range.

At high speeds the main criteria of performance are the drag critical Mach number and the maximum Mach number. Fig. 14 shows that the former decreases steadily as the position of maximum camber is brought forward. The reflex in the test curve is due to the fact that with these cascades, the lift coefficient is also a function of the position of maximum camber. When the curve has been corrected to a constant value of the lift coefficient there is a steady and appreciable decline as shown by the dotted curve in Fig. 14. It would seem desirable on this account to have the position of maximum camber as far back as possible.

Comparison of the maximum Mach number at maximum lift/drag conditions is not a true criterion since it usually occurs in a compressor at low incidences. Unfortunately the negative shift of the working range somewhat obscures the performance at these points. It would seem fairly definite, however, that blades with the position of maximum camber near the leading edge will have higher choking mass flows on account of the larger throat area associated with this type of camber line.

To summarise these results, then, it would appear that

(1) Blades with their position of maximum camber in the rearward position will give

- (a) a high work capacity,
- (b) a high efficiency,
- (c) a high drag critical Mach number.

(2) Blades with their position of maximum camber in a forward position give

- (a) a larger working range,
- (b) a higher choking mass flow.

5.3. *Comparison with Previous Work.*—Previous work on this subject has been reported in Refs. 1, 2 and 4 though in all cases it has been confined to a comparison of blades with circular-arc camber lines and parabolic camber lines with the position of maximum camber 40 per cent from the leading edge. Refs. 1 and 4 contain test results which are in general agreement with those reported here.

In Ref. 1, aerodynamically equivalent cascades were tested at low speeds only. The conclusions were in favour of the parabolic blading ($a/c = 40$ per cent) on the grounds of greater working range and greater throat area. The more negative incidence of the working point with this type of blading does not appear large in these tests, and is ignored in the conclusions. Actually the magnitude could be attributed to experimental error, but has been made much smaller by smooth curves drawn through test points taken at wide incidence intervals.

In Ref. 4 geometrically similar blades were tested at all speeds up to choking. As the blades were not aerodynamically equivalent direct comparison is not possible, but the conclusions reached were (a) the working range was the same for both blades tested, (b) the circular-arc cambered blades had a 5 deg higher working incidence, (c) the circular-arc blade had a higher drag critical Mach number, and (d) the parabolic blade had a higher choking mass flow. These results are, with the exception of (a) above, in general agreement with the results presented in this report.

To a certain extent the results just referred to had been anticipated by the theoretical analysis of R. & M. 2384[2]. It was shown there that greater upper surface suction peaks were associated with blades having their maximum camber near the leading edge, due of course to the larger curvature in that region with this type of blade. Such pressure distributions were associated with a large working range and a low critical Mach number, and consequently it was argued in R. & M. 2384[2], a low drag critical Mach number. It has since been pointed out, however[5], that a low critical Mach number does not necessarily imply a low-drag critical Mach number, the behaviour at Mach numbers above the critical itself being a function of the pressure distribution. Again, some cascade tests reported in Ref. 6 indicate that the drag critical Mach number is some 13 to 16 per cent higher than the critical Mach number, but depending, in these tests, on the pitch/chord ratio rather than the pressure distribution. Considerable doubt seems to exist concerning the best form the pressure distribution should take, though some later work on isolated aerofoils[7,8,9] has suggested that the position of maximum suction should be kept as far back as possible, this time on the grounds that when transonic flow does take place the limitation of the supersonic region ahead of the shock will not be excessive.

Finally it must be emphasised that the results and comments on them apply to the two-dimensional cascade performance. In a compressor, miscellaneous secondary flows may well have a controlling effect on the performance of blade sections, and this should not be lost sight of in applying cascade test results to compressors.

6. *Conclusions.*—From the test results and general discussion given in this report the following conclusions appear justified.

(1) Bringing the position of maximum camber forward gives a wider working range and a higher choking mass flow.

(2) Moving the position of maximum camber back gives a higher work capacity and a higher drag critical Mach number.

(3) With the present design rule there can be no doubt that the best all-round performance is obtained with blades having the position of maximum camber 50 per cent of the chord from the leading edge, provided adequate throat area can be provided with this design.

(4) With improved methods of design it is anticipated that the performance of the other positions of the maximum camber could be improved, but even so the best combination of large working range and good high-speed performance appears to occur for a blade having its position of maximum camber as in section 6.3 above.

These conclusions apply to the two-dimensional performance of a cascade of blades: in an actual compressor the results may have to be modified to accommodate the three-dimensional nature of the flow.

7. *Acknowledgments.*—The author is indebted to Messrs. E. Duncombe and N. A. Dimmock, and to Miss H. Hughes for their share of the experimental and computation work involved.

REFERENCES

No.	Author	Title, etc.
1	A. R. Howell	A Note on the Compressor Base Aerofoils C.1, C.2, C.3, C.4, C.5, and Aerofoils made up of Circular Arcs. Power Jets (R. & D.), Ltd. Memorandum No. M.1011. September, 1944.
2	A. D. S. Carter and Hazel P. Hughes	A Theoretical Investigation into the Effect of Profile Shape on the Performance of Aerofoils in Cascade. R. & M. 2384. March, 1946.
3	A. R. Howell	The Present Basis of Axial Flow Compressor Performance, Pt. I. Cascade Theory and Performance. R. & M. 2095. June, 1942.
4	S. J. Andrews, Patricia M. Andrews and Margaret Baines.	A Comparison between Two Compressor Cascades using C.4 Profile on Parabolic and Circular Arc Camber Lines. A.R.C. Report 10,267. September, 1946. (Unpublished.)
5	J. S. Thompson and W. A. Mair (Editor Prof. A. Thom).	The R.A.E. High Speed Tunnel and a Review of the Work Accomplished in 1942–5. R. & M. 2222. September, 1946.
6	Seymour M. Bogdonoff	N.A.C.A. Cascade Data for the Blade Design of High Performance Axial Flow Compressors. *J. Ae. Sci.*, Vol. 15, No. 2. February, 1948.
7	F. N. Kirk	Effects of Mach Number on Maximum Lift. A.R.C. Report 10,463. January, 1947. (Unpublished.)
8	J. A. Beavan, R. Sargent and Miss B. Burrows.	Measurement of Maximum Lift on 19 Aerofoil Sections at High Mach Numbers. R. & M. 2678. January, 1948.
9	J. A. Beavan and R. Hills	Maximum Lift Coefficients of Aerofoil Sections at High Subsonic Mach Numbers. A.R.C. Report 11,102. December, 1947. (Unpublished.)

APPENDIX I

Aerofoil Nomenclature

The same aerofoil nomenclature has been used as by Howell[3]. The following is an example

10 C1/40 C50

where 10 is the maximum thickness in per cent chord, C1 denotes base profile, 40 is the camber angle in degrees, C denotes a circular-arc camber line, and 50 is the distance of the point of maximum camber from the leading edge in per cent chord. Sometimes a parabolic camber line is used, which is denoted by P.

APPENDIX II

TABLE 2

Cascade 10C4/31·5 P30 $\zeta = -17\cdot2°$ $s/c = 1\cdot0$

$\alpha_1 = 21\cdot7$ deg ($i = -22\cdot9$ deg)

M_1	0·294	0·378	0·460	0·565	0·662	0·732
ε	7·7	7·4	7·6	7·5	8·1	8·1
$\varpi/P_{tot\,1} - P_{stat\,1}$	0·024	0·027	0·026	0·035	0·049	0·064
$\Delta P/P_{tot\,1} - P_{stat\,1}$	0·019	0·025	0·021	0·021	0·019	−0·008
M_2	0·292	0·376	0·450	0·557	0·653	0·735
$\varpi/P_{tot\,2} - P_{stat\,2}$	0·025	0·028	0·026	0·036	0·050	0·063

$\alpha_1 = 25\cdot7$ deg ($i = -18\cdot9$ deg)

M_1	0·290	0·385	0·471	0·580	0·685	0·757
ε	11·0	11·1	11·2	11·1	10·9	9·4
$\varpi/P_{tot\,1} - P_{stat\,1}$	0·017	0·018	0·021	0·023	0·039	0·092
$\Delta P/P_{tot\,1} - P_{stat\,1}$	0·058	0·062	0·064	0·069	0·067	−0·011
M_2	0·289	0·371	0·456	0·558	0·657	0·762
$\varpi/P_{tot\,2} - P_{stat\,2}$	0·019	0·019	0·023	0·025	0·042	0·092

$\alpha_1 = 31\cdot2$ deg ($i = -13\cdot4$ deg)

M_1	0·305	0·395	0·488	0·610	0·702	0·780
ε	16·2	16·4	16·3	16·4	15·9	13·3
$\varpi/P_{tot\,1} - P_{stat\,1}$	0·020	0·023	0·025	0·030	0·068	0·129
$\Delta P/P_{tot\,1} - P_{stat\,1}$	0·019	0·094	0·122	0·131	0·099	0·003
M_2	0·289	0·373	0·454	0·558	0·657	0·776
$\varpi/P_{tot\,2} - P_{stat\,2}$	0·022	0·026	0·028	0·035	0·076	0·130

$\alpha_1 = 34\cdot0$ deg ($i = -10\cdot6$ deg)

M_1	0·314	0·408	0·500	0·613	0·694	0·783
ε	18·4	18·4	18·5	18·2	16·4	14·1
$\varpi/P_{tot\,1} - P_{stat\,1}$	0·036	0·036	0·040	0·057	0·118	0·164
$\Delta P/P_{tot\,1} - P_{stat\,1}$	0·138	0·143	0·147	0·136	0·075	−0·016
M_2	0·292	0·373	0·458	0·559	0·658	0·787
$\varpi/P_{tot\,2} - P_{stat\,2}$	0·043	0·043	0·047	0·067	0·129	0·163

$\alpha_1 = 36\cdot7$ deg ($i = -7\cdot9$ deg)

M_1	0·319	0·412	0·494	0·590	0·681	0·768
ε	19·8	19·7	18·5	16·8	16·0	14·1
$\varpi/P_{tot\,1} - P_{stat\,1}$	0·054	0·057	0·089	0·162	0·194	0·229
$\Delta P/P_{tot\,1} - P_{stat\,1}$	0·158	0·146	0·133	0·087	0·050	0·004
M_2	0·284	0·370	0·447	0·555	0·653	0·762
$\varpi/P_{tot\,2} - P_{stat\,2}$	0·066	0·068	0·105	0·182	0·209	0·233

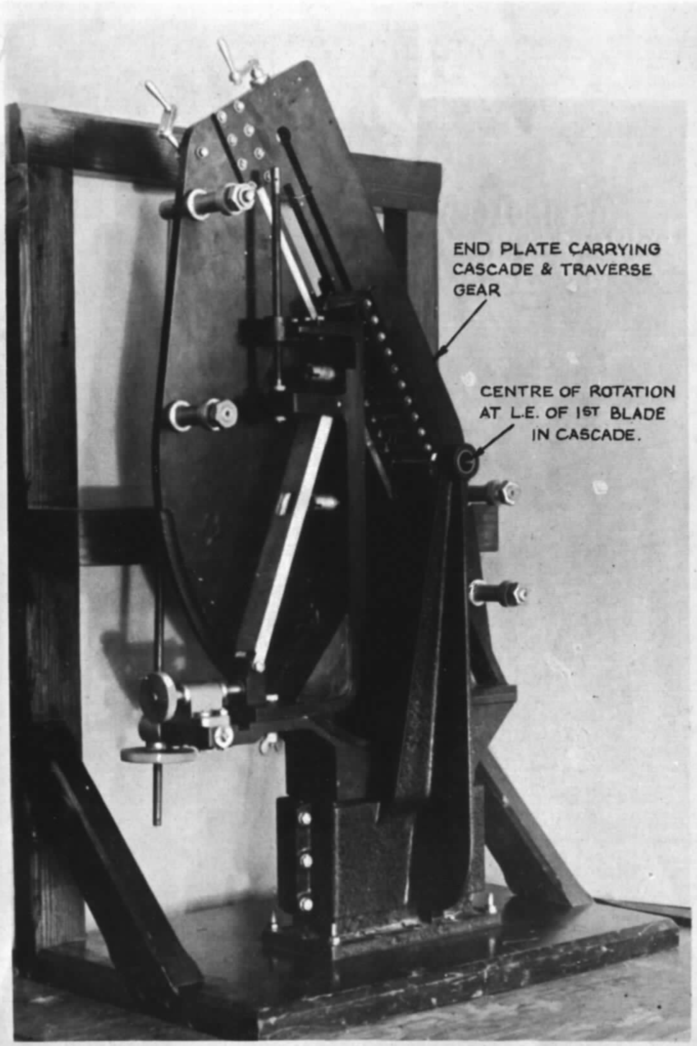

FIG. 1a. View with one end-plate removed showing cascade in position, and adjustable side wall.

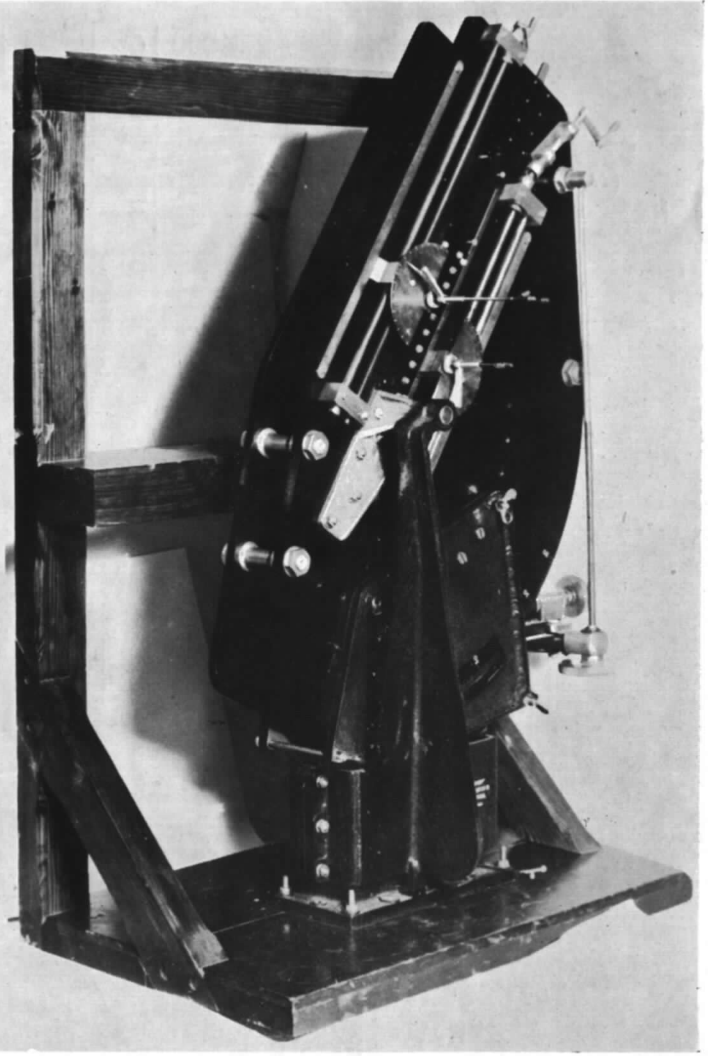

FIG. 1b. View showing complete assembly and traversing gear.

No. 6 High Speed Cascade Tunnel.

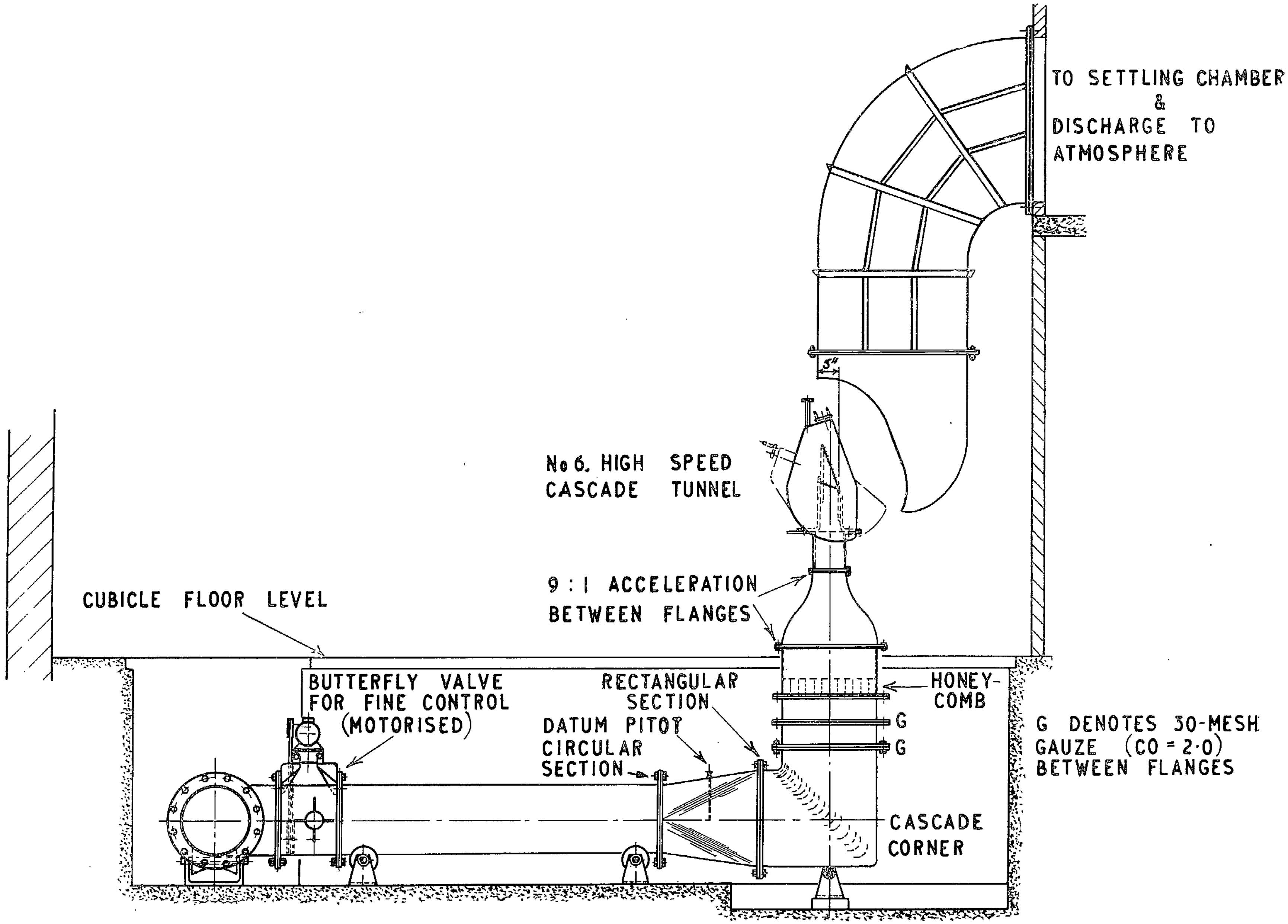

FIG. 2. Installation of No. 6 Tunnel in No. 6 Cubicle.

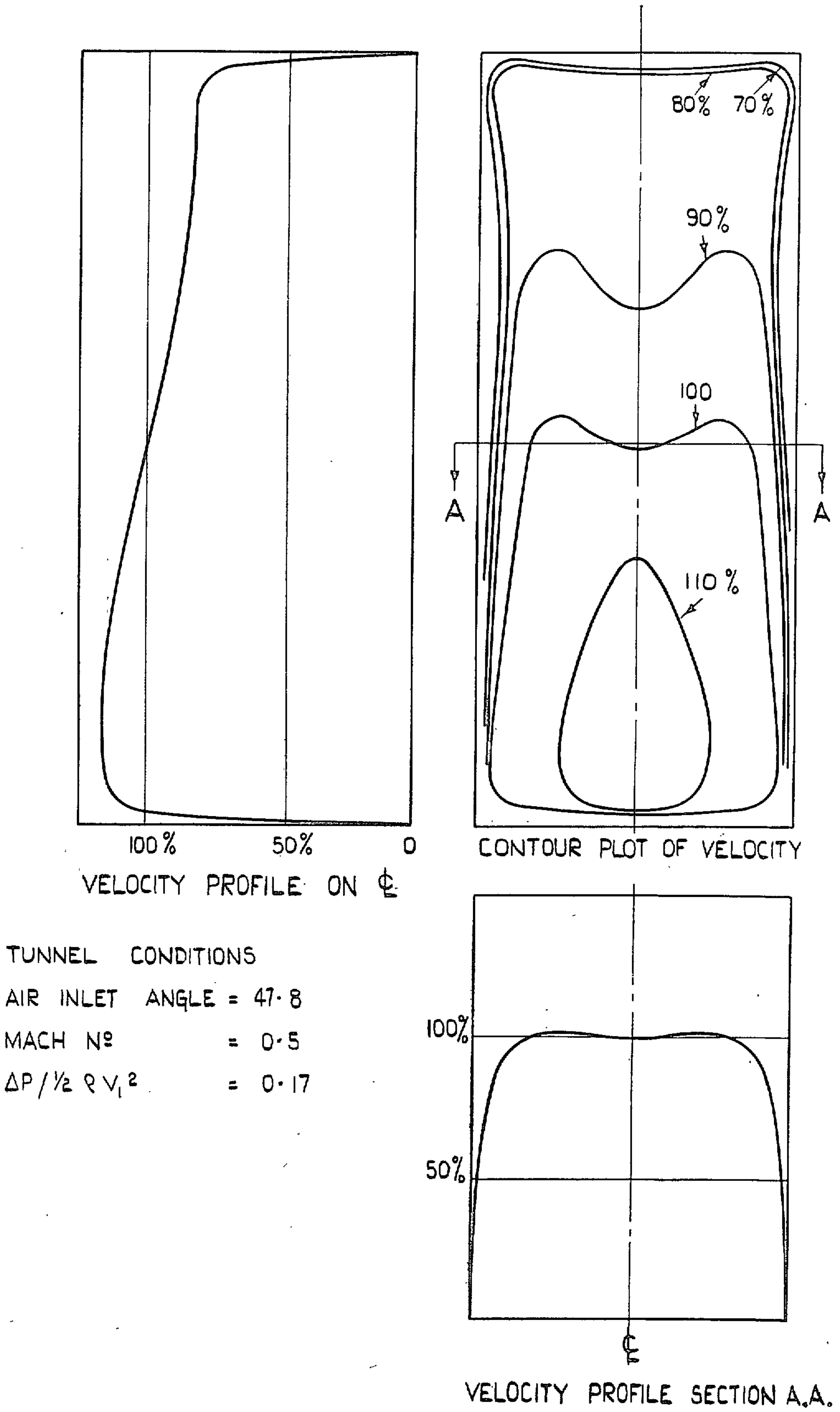

FIG. 3. Inlet velocity profile. (Velocities expressed as percentage of datum velocity.)

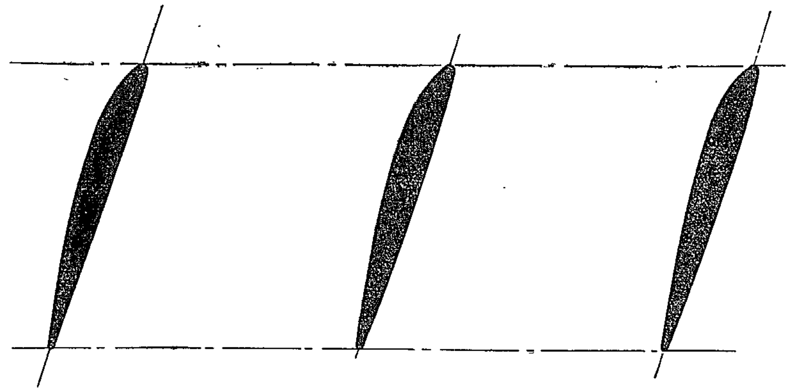

AEROFOIL 10C4/31·5 P 30
STAGGER - 17·2°
PITCH/CHORD 1·0

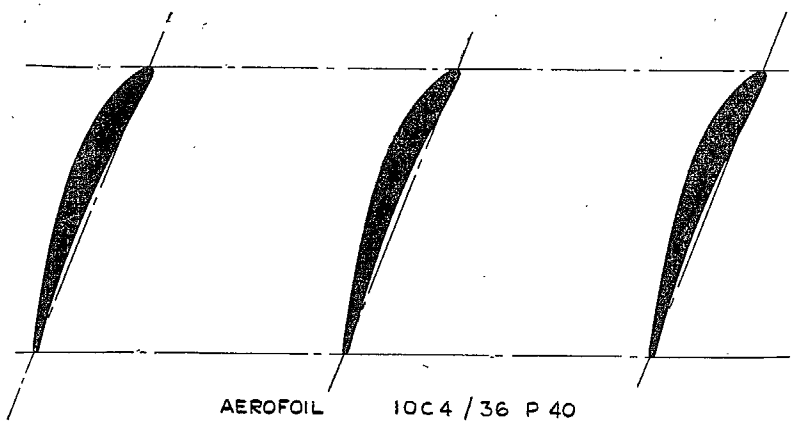

AEROFOIL 10C4/36 P 40
STAGGER - 21·4°
PITCH/CHORD 1·0

FIG. 4. Cascades.

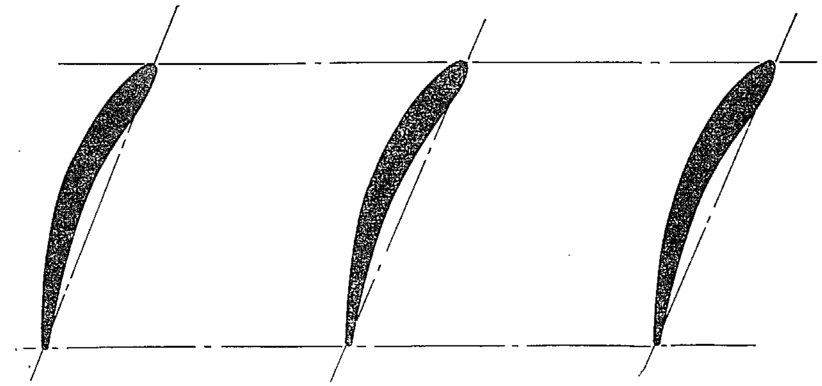

AEROFOIL 10C4/40 P 50
STAGGER - 24·9°
PITCH/CHORD 1·0

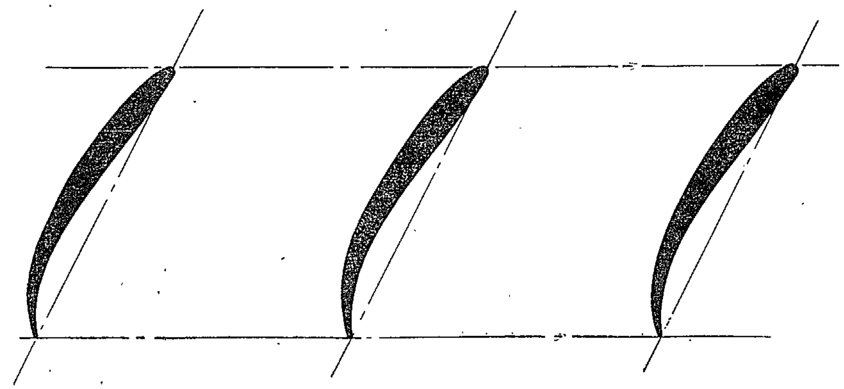

AEROFOIL 10C4/51 P 60
STAGGER - 28·7°
PITCH/CHORD 1·0

FIG. 5. Cascades.

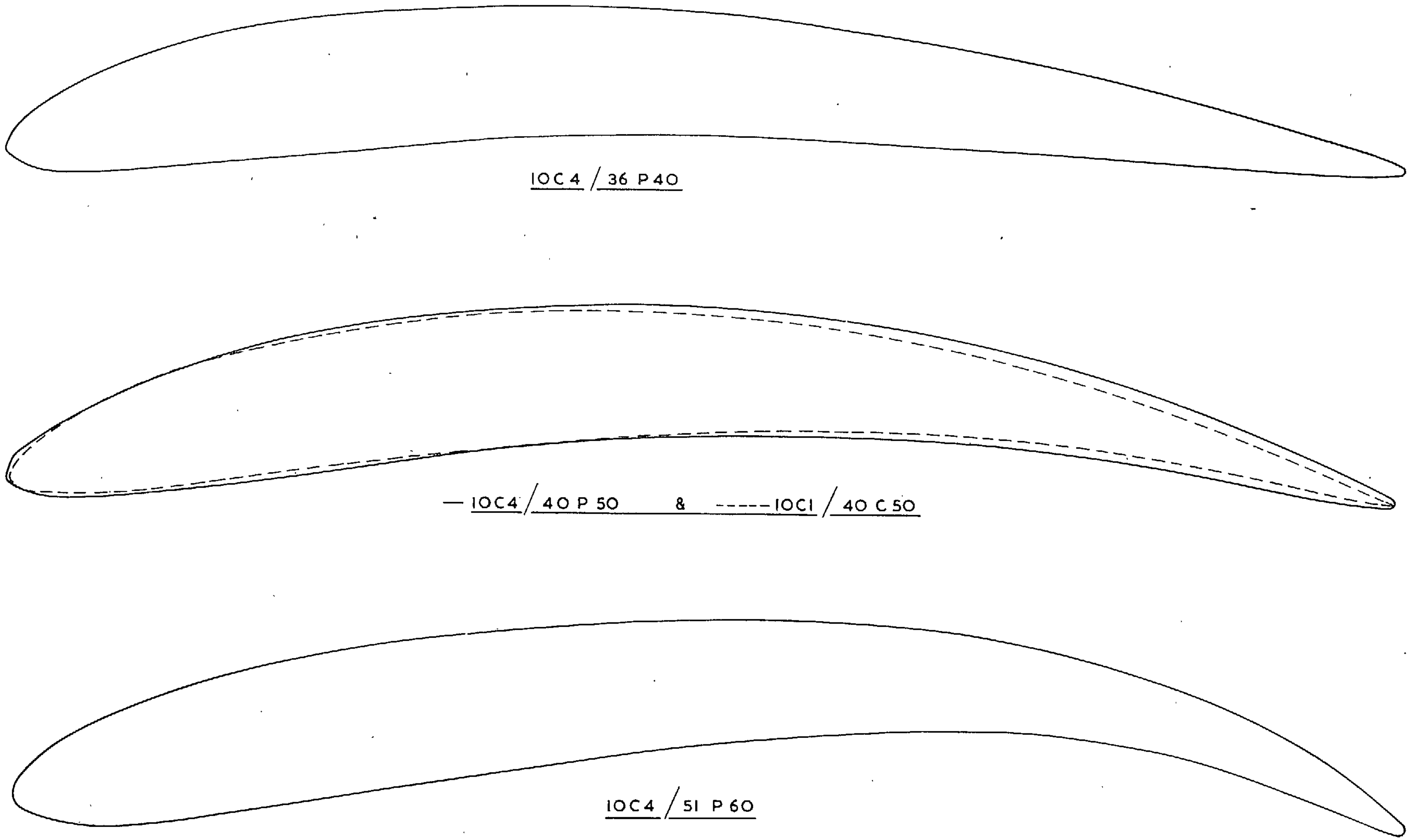

Fig. 6. Enlarged blade profiles.

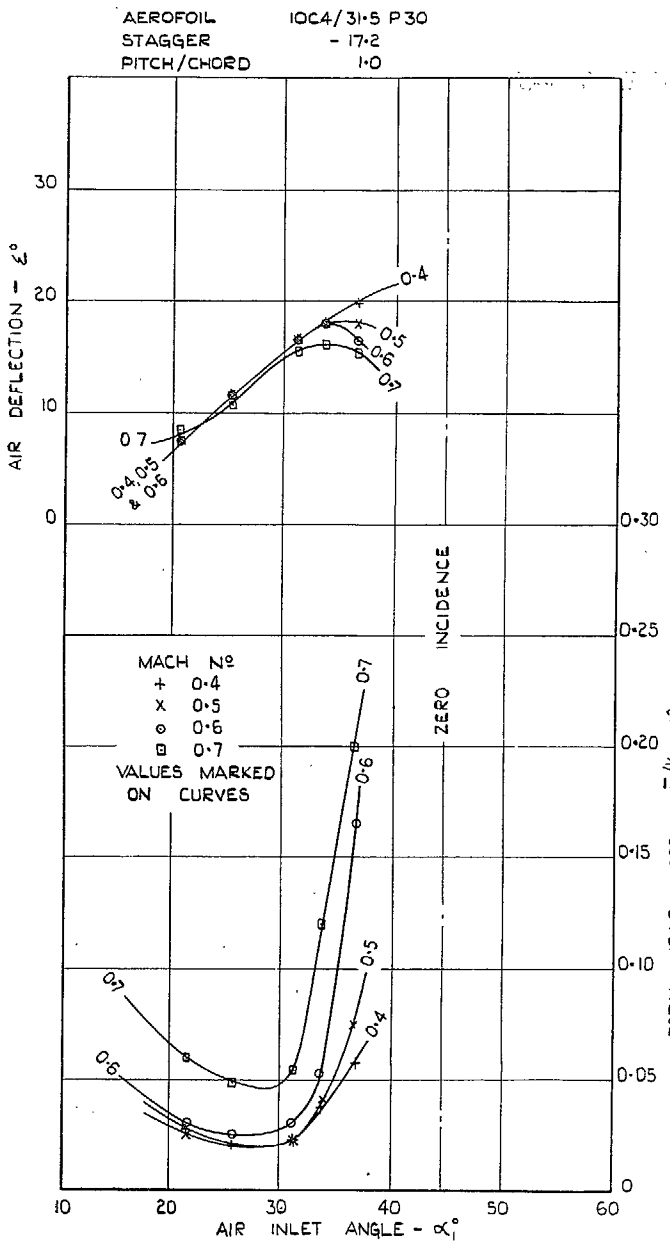

FIG. 7. Cascade characteristics.

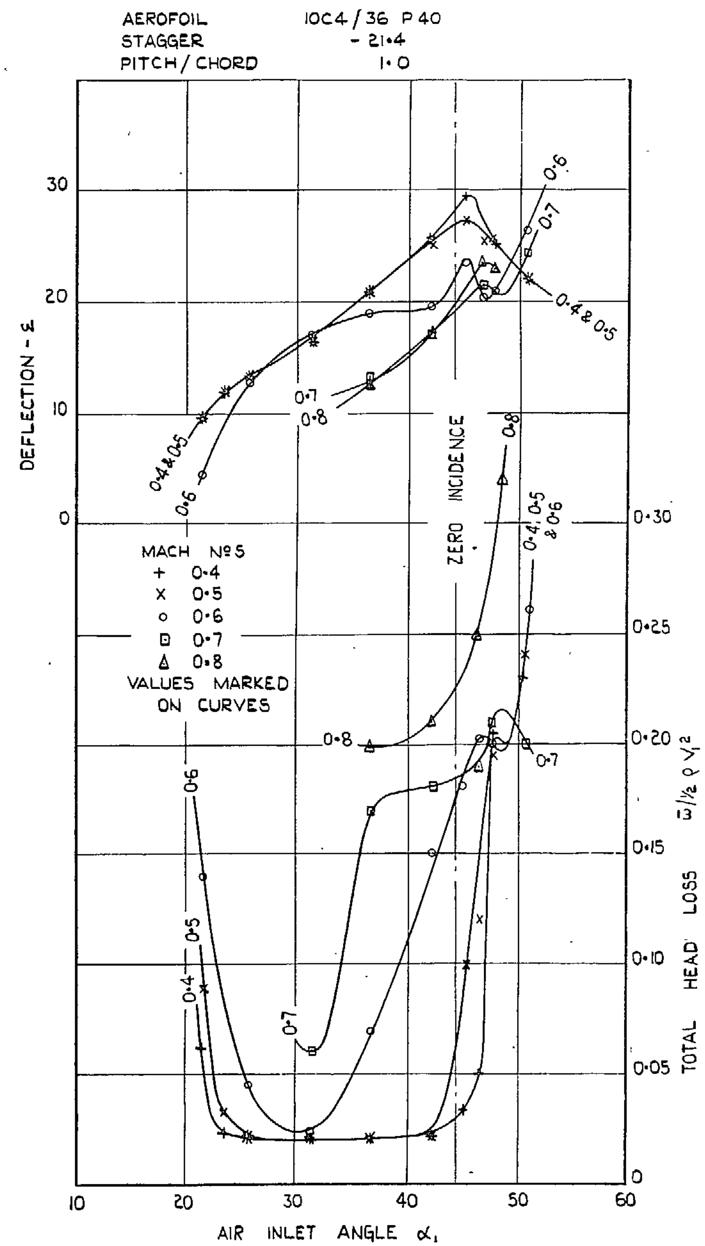

Fig. 8. Cascade characteristics.

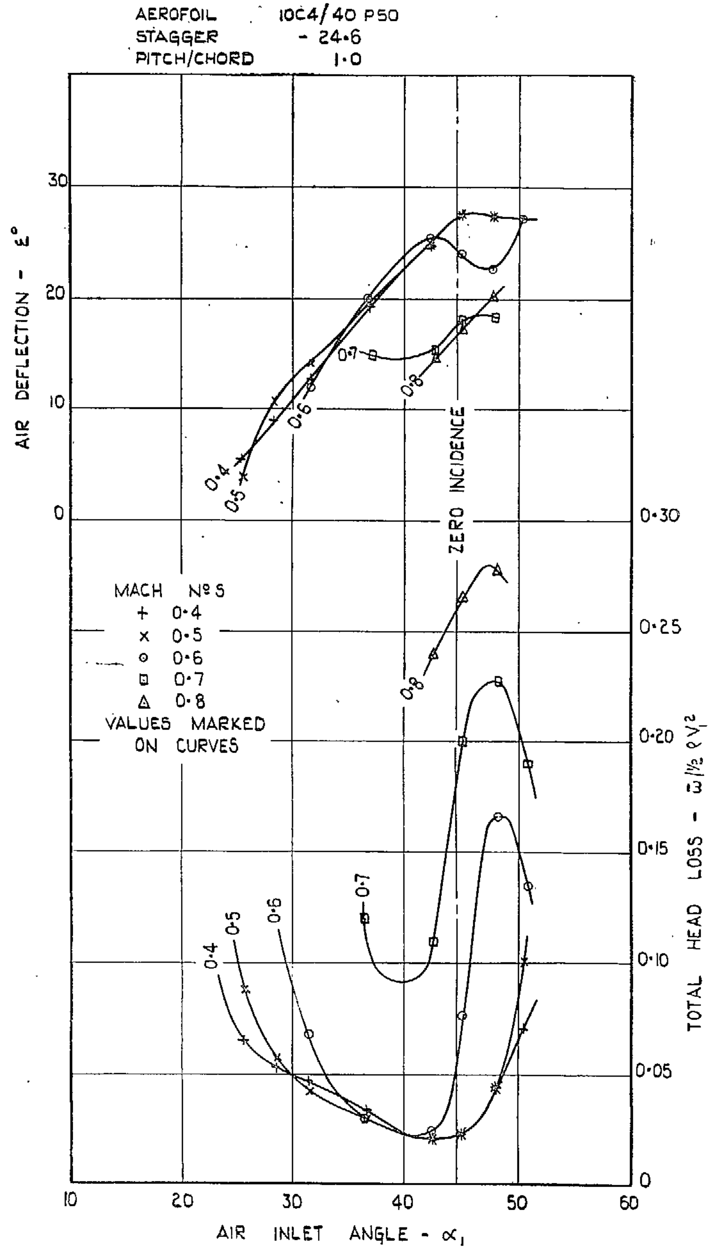

FIG. 9. Cascade characteristics.

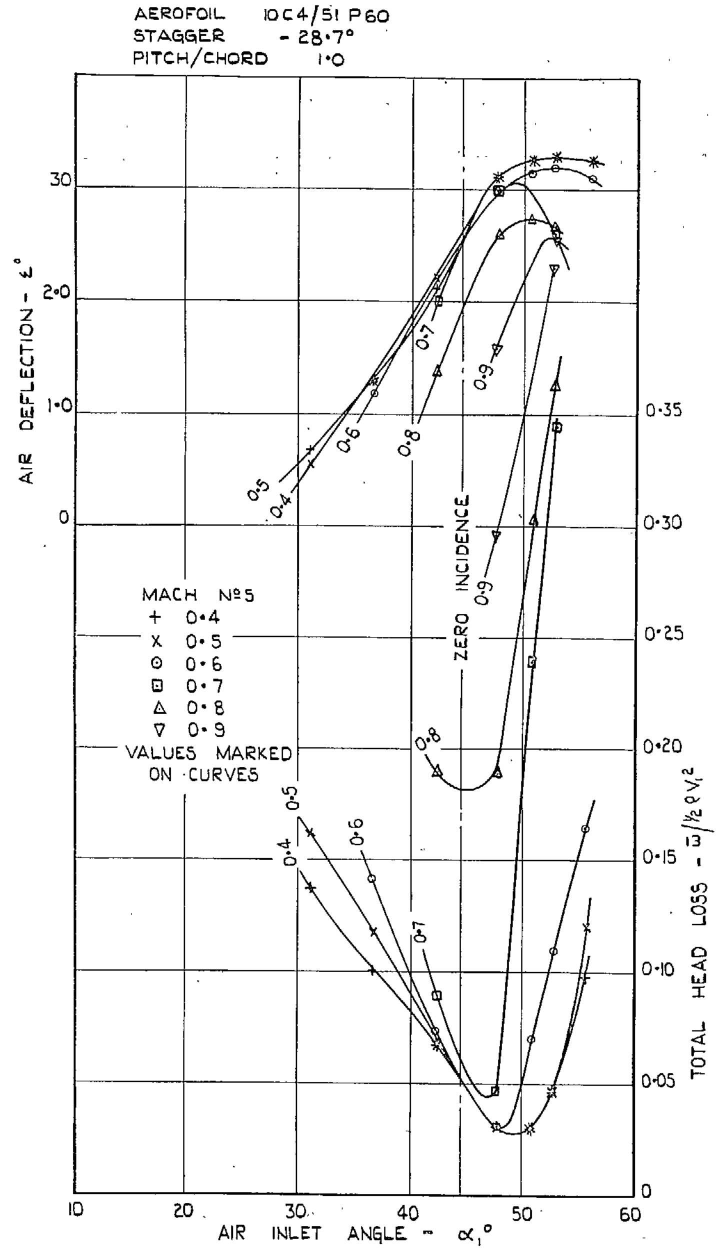

FIG. 10. Cascade characteristics.

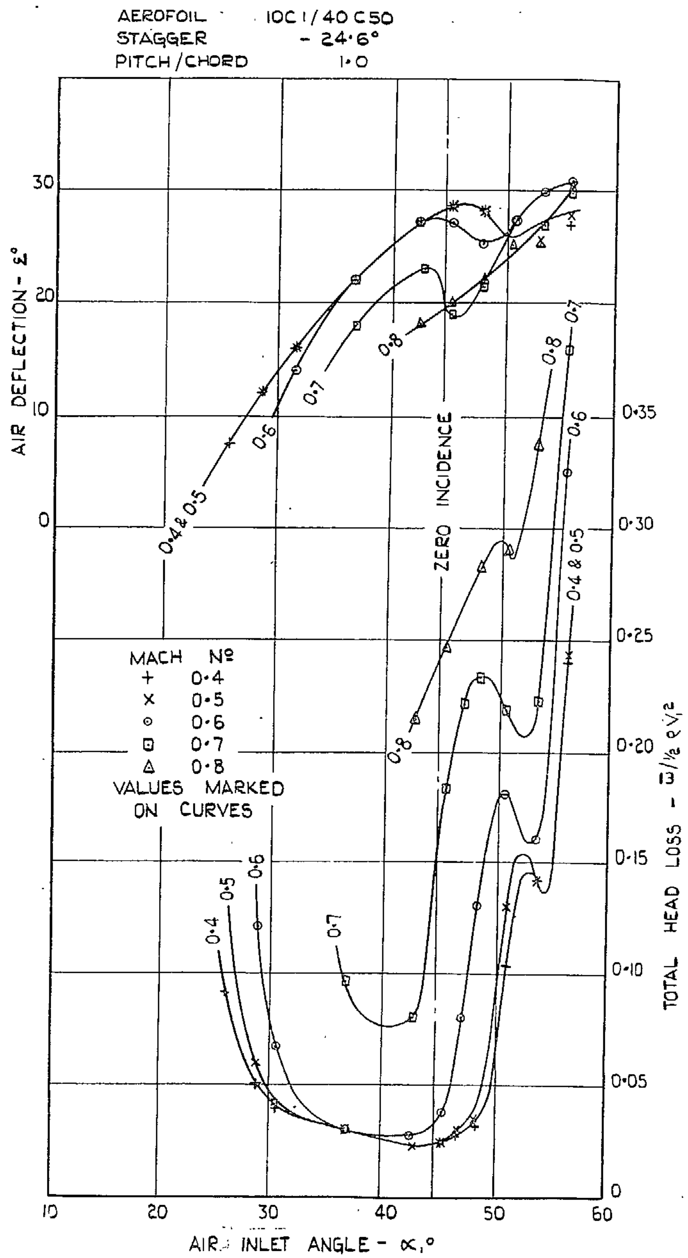

FIG. 11. Cascade characteristics.

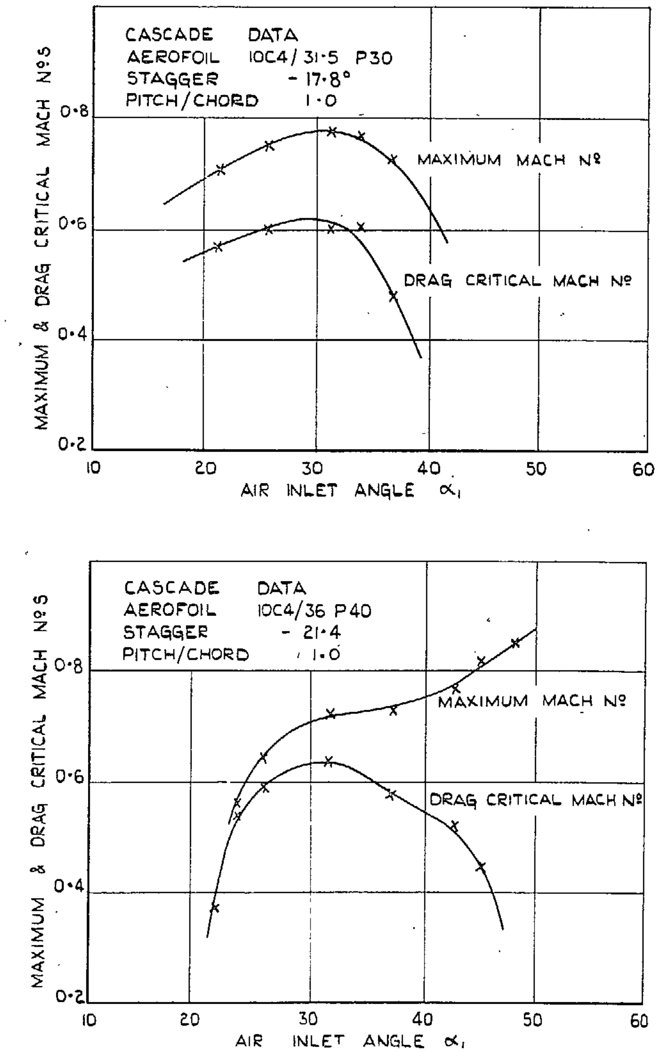

FIG. 12. Maximum and drag critical Mach numbers.

Maximum Mach number—Zero pressure rise across cascade. Drag critical Mach number.
Loss $= 1 \cdot 5 \times$ minimum loss at const. incidence.

(52207) Wt. 15/680 K.9 5/53 Hw.

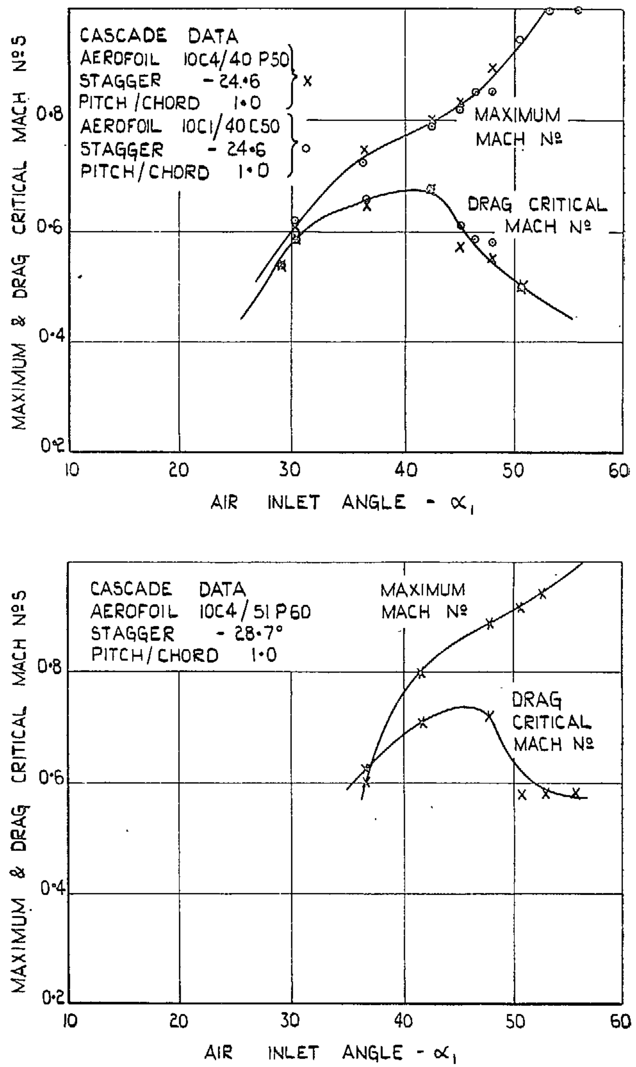

FIG. 13. Maximum and drag critical Mach number. Maximum Mach number—Zero pressure rise across cascade. Drag critical Mach number. Loss = $1 \cdot 5 \times$ minimum loss at const. incidence.

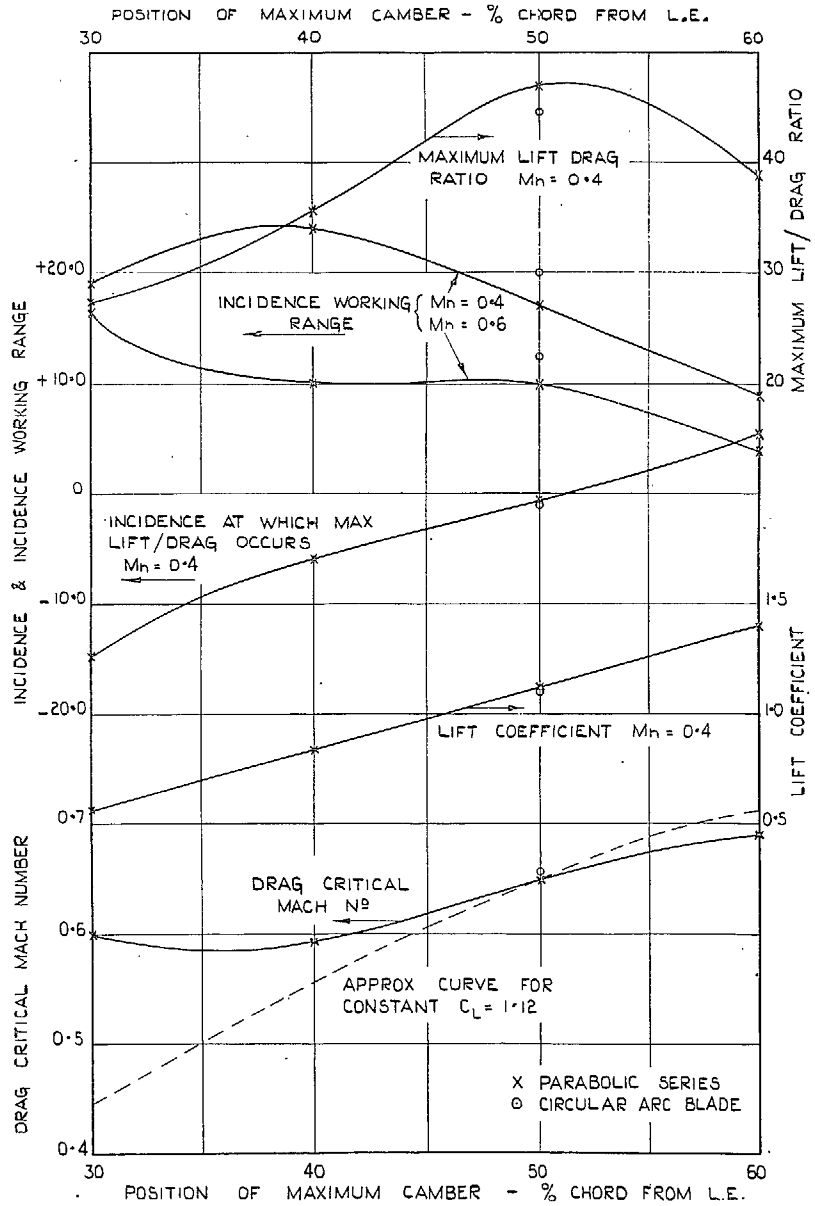

FIG. 14. Conditions at working point for various positions of maximum camber.

PRINTED IN GREAT BRITAIN

R. & M. No. 2694
(12,324)
A.R.C. Technical Report

Publications of the Aeronautical Research Council

ANNUAL TECHNICAL REPORTS OF THE AERONAUTICAL RESEARCH COUNCIL (BOUND VOLUMES)

1936 Vol. I. Aerodynamics General, Performance, Airscrews, Flutter and Spinning. 40s. (40s. 9d.)
Vol. II. Stability and Control, Structures, Seaplanes, Engines, etc. 50s. (50s. 10d.)

1937 Vol. I. Aerodynamics General, Performance, Airscrews, Flutter and Spinning. 40s. (40s. 10d.)
Vol. II. Stability and Control, Structures, Seaplanes, Engines, etc. 60s. (61s.)

1938 Vol. I. Aerodynamics General, Performance, Airscrews. 50s. (51s.)
Vol. II. Stability and Control, Flutter, Structures, Seaplanes, Wind Tunnels, Materials. 30s. (30s. 9d.)

1939 Vol. I. Aerodynamics General, Performance, Airscrews, Engines. 50s. (50s. 11d.)
Vol. II. Stability and Control, Flutter and Vibration, Instruments, Structures, Seaplanes, etc. 63s. (64s. 2d.)

1940 Aero and Hydrodynamics, Aerofoils, Airscrews, Engines, Flutter, Icing, Stability and Control, Structures, and a miscellaneous section. 50s. (51s.)

1941 Aero and Hydrodynamics, Aerofoils, Airscrews, Engines, Flutter, Stability and Control, Structures. 63s. (64s. 2d.)

1942 Vol. I. Aero and Hydrodynamics, Aerofoils, Airscrews, Engines. 75s. (76s. 3d.)
Vol. II. Noise, Parachutes, Stability and Control, Structures, Vibration, Wind Tunnels. 47s. 6d. (48s. 5d.)

1943 Vol. I. (*In the press.*)
Vol. II. (*In the press.*)

ANNUAL REPORTS OF THE AERONAUTICAL RESEARCH COUNCIL—

1933–34	1s. 6d. (1s. 8d.)	1937	2s. (2s. 2d.)
1934–35	1s. 6d. (1s. 8d.)	1938	1s. 6d. (1s. 8d.)
April 1, 1935 to Dec. 31, 1936.	4s. (4s. 4d.)	1939–48	3s. (3s. 2d.)

INDEX TO ALL REPORTS AND MEMORANDA PUBLISHED IN THE ANNUAL TECHNICAL REPORTS, AND SEPARATELY—

April, 1950 - - - - R. & M. No. 2600. 2s. 6d. (2s. 7½d.)

AUTHOR INDEX TO ALL REPORTS AND MEMORANDA OF THE AERONAUTICAL RESEARCH COUNCIL—

1909–1949. R. & M. No. 2570. 15s. (15s. 3d.)

INDEXES TO THE TECHNICAL REPORTS OF THE AERONAUTICAL RESEARCH COUNCIL—

December 1, 1936 — June 30, 1939.	R. & M. No. 1850.	1s. 3d. (1s. 4½d.)
July 1, 1939 — June 30, 1945.	R. & M. No. 1950.	1s. (1s. 1½d.)
July 1, 1945 — June 30, 1946.	R. & M. No. 2050.	1s. (1s. 1½d.)
July 1, 1946 — December 31, 1946.	R. & M. No. 2150.	1s. 3d. (1s. 4½d.)
January 1, 1947 — June 30, 1947.	R. & M. No. 2250.	1s. 3d. (1s. 4½d.)
July, 1951.	R. & M. No. 2350.	1s. 9d. (1s. 10½d.)

Prices in brackets include postage.

Obtainable from

HER MAJESTY'S STATIONERY OFFICE

York House, Kingsway, London, W.C.2; 423 Oxford Street, London, W.1 (Post Orders: P.O. Box 569, London, S.E.1); 13a Castle Street, Edinburgh 2; 39, King Street, Manchester, 2; 2 Edmund Street, Birmingham 3; 1 St. Andrew's Crescent, Cardiff; Tower Lane, Bristol 1; 80 Chichester Street, Belfast, or through any bookseller

S.O. Code No. 23-2694